# Test Beds for integrated transmission and distribution networks: Generation methodology and benchmarks

Jing Yu, *Student Member, IEEE*, Ye Guo, *Senior Member, IEEE*, Hongbin Sun, *Fellow, IEEE*

***Abstract*— For future power systems with high penetration of distributed energy resources (DERs), the coordination of transmission system (TS) and distribution systems (DSs) is quite essential. In this paper, multiple testbeds that consist of various sizes of TS and DS models are designed for power flow (PF) and optimal power flow (OPF) analysis of the integrated transmission and distribution (T&D) systems. Several benchmarks with characteristics on applications are proposed and their simulation results are also presented in this paper. Researchers can use the testbeds designed in this paper to build their specific cases with published data, and can also compare the results of their new approaches or algorithms with those obtained by the proposed benchmarks in this paper.**

***Index Terms*—Test system design, multi-area power systems, transmission system, distribution system, optimal power flow.**

## I. INTRODUCTION

### A. Background

Since the penetration level of distributed energy resources (DERs) is increasing at the distribution level, the outdated image that transmission system (TS) hosts the supply side while the distribution system (DS) hosts the demand side is experiencing dramatic changes. With the increasing amount of distributed resources, the stakeholders at the distribution level are no longer pure consumers and can provide services for the overall benefit of the power system. Hence, in order to enhance the security, competitiveness and sustainability of the entire power systems, the arrangements between transmission system operator (TSO) and distribution system operators (DSOs) need to be revised and developed further to coordinately play a more active role in the following points:

1) Exploring the flexibility in the distribution side to avoid the transformer congestion between TS and DSs.
2) Managing the transmission line overload in TS through integrating DERs into DSs.
3) Reducing the boundary imbalance caused by fluctuated distributed generations through TSO-DSO cooperation.
4) Activating local flexibility to support voltage of each other and enabling the coordinated protection.

There are lots of evidences from policy to industry to support the conclusion that in future power systems with high-level DER penetrations, TSO-DSO coordination will become one of the key techniques [1]-[9]. For example, the agency for the cooperation of energy regulation (ACER) has published a report to improve the coordination between TSOs and DSOs [10]. Also, the European Commission published a report that addressed there is a need for more coordination between the TSOs and DSOs, especially under the interconnection of smart grids operating in different EU Member State [11]. At the same time, lots of demonstration projects across the world concentrated on enhancing DSO-TSO cooperation. For instance, the SMARTNET project has analyzed potential DSO-TSO coordination schemes [12]. Coincidentally, the Council of European Energy Regulators (CEER) not only focused on the future DSO-TSO relationship, but also related regulatory arrangements regarding planning and operation [13].

Moreover, TSO-DSO coordination has also drawn extensive concern in the academic in recent years. A series of research efforts have substantiated the necessity and benefits of TSO-DSO coordination [14]-[21]. The topics vary from the global power flow solution [14], optimal power flow [15] and coordinated economic dispatch [16]-[18], to security analysis [19][20] and hierarchical reactive power optimization [21], etc. These investigations have widely facilitated the development of studies for TSO-DSO coordination.

However, one visible problem is that the comparisons between different approaches are still a non-trivial task due to the lack of widely accepted test systems. That means in most cases, the freely-designed test systems designed for specific problems are challenging to be applied in other applications. Although there are some specific test models designed for analyzing the TSO-DSO interactions, such as the small-scale transmission and distribution (T&D) test system that consists of a six-bus TS and two active DS in [22]. Beyond that, a series of open-source, parametrizable T&D test models can be generated by a MATLAB toolbox named TDNetGen [23][24]. However,

This work was supported in part by the National Key Research and Development Program of China under Grant 2018YFB0905000, in part by the National Natural Science Foundation of China (NSFC) under Grant 51537006, and in part by the Science, Technology and Innovation Commission of Shenzhen Municipality under Grant JCYJ20170411152331932.

Jing. Yu and Ye. Guo are with the Shenzhen Environmental Science and New Energy Technology Engineering Laboratory Tsinghua-Berkeley Shenzhen Institute, Tsinghua University Shenzhen, China.

Hongbin. Sun is with the State Key Laboratory of Power Systems, Department of Electrical Engineering, Tsinghua University, Beijing 100084, China (Corresponding author: Hongbin Sun, shb@tsinghua.edu.cn).

the common deficiency of the aforementioned T&D test models is that the choice of the separated model for TS and DS is simple and limited. For example, only one scale of DS is provided in TDNetGen, thus, it is difficult to represent the heterogeneity of different DSs. Therefore, for the reasons mentioned above, up to now, when researchers investigate the interplay between TS and DS or examine the specified algorithms designed for the co-operation or co-planning for TSO and DSO, there is a lack of combined T&D benchmarks available for all the applications.

### B. Contributions and Organization

In this paper, several testbeds for TS and DS varying in scale and load level are selected to build the T&D benchmarks for TSO-DSO coordination analysis. The data is provided in the template of MATPOWER, so researchers can freely generate various-size T&D test models for a variety of studies. In the meantime, it is possible to compare the performances of the newly proposed methods or algorithms against the existing ones relying on these publicly accessible data.

The two primary purposes of this paper can be summarized as follows:

1) The first goal is to provide several separated TS and DS models, based on which, highly-customizable T&D testbeds can be built and enlarged by replacing the aggregated loads of TS by detailed DSs with similar load levels.
2) The second purpose is to provide four T&D benchmarks. The effectiveness of these systems is verified by figuring out reasonable power flow and optimal power flow solutions. The parameters and detailed results are provided to perform as reference for similar researches.

The remainder of this paper is organized as follows. In Section II, the basics of generating integrated T&D systems are introduced. Section III gives the distributed model of optimal power flow for the integrated system. Then, In Section IV, the results of the comparison between the distributed model and MATPOWER for some example testbeds are provided. Finally, some concluding remarks are presented in Section VI.

## II. Integrated T&D System Generation

In the real power grid, a TS is generally connected with several DSs, so the newly generated integrated T&D systems are composed of one TS and several DSs. The TS and DS models, as well as the generation process of the combined T&D systems, are introduced in the remainder of this section.

### A. Description of TS and DS models

#### 1) TS Models

Four typical TS models are used for generating the T&D benchmarks, as in TABLE I from small to large scale.

TABLE I
Summary of TS Models

| TS | Bus. | Bran. | Gen. | P (MW) | Q (MVAR) |
|---|---|---|---|---|---|
| T6 [22] | 6 | 7 | 3 | 183.000 | 52.000 |
| T30 [25] | 30 | 41 | 6 | 189.200 | 107.200 |
| T57 [25] | 57 | 80 | 7 | 1295.400 | 362.900 |
| T118 [25] | 118 | 186 | 54 | 4242.000 | 1438.000 |

For the smallest one, a meshed 6-bus TS model is designed based on that proposed in [22]. Then, all the other TS models are widely-used IEEE test systems, which have already been published and provided in the data set of the latest version of MATPOWER.7.0b1 [25]. The basic information for these TS models, including the number of buses (Bus), branches (Bran.) and generators (Gen.), are summarized in TABLE I. Also, the total active (P) and reactive power (Q) delivered to the demands are also given.

#### 2) DS Models

The models for DS varying in topology and load levels are given in TABLE II. First, the smallest two DS models, i.e., D7 and D9, are modified based on the DSs proposed in [22], which consist of 7 buses and 9 buses, respectively. The demand level of these two systems are relatively high, representing the DSs that are seeing a rapid growth of internal demand in recent years [26]. D33 is the widely-used radial 33-bus DS case [27]. Each DS model mentioned above consists of a single feeder. The fourth DS model DF3 is the three-feeder DS model provided in [28], and the tie-switches between the radial feeders are normally opened. Another looped 6-feeder DS model, called DF6, is modified base on the 44kV DS provided by the Kingston public utility commission [29]. This model characterizes the area, wherein light industrial, commercial and civil load co-exist. Finally, an 8-feeder and 76-bus system is adopted, which is modified based on the 75-buses distribution network provided by the Centre for Sustainable Electricity and Distributed Generation (SEDG) [24].

In addition to the scale information, the base voltage and load level of the DS models are summarized in TABLE II.

TABLE II
Summary of DS Models

| DS | Bus. | Bran. | Feeder. | Vbase (kV) | Load level (MW) | Load level (MVar) |
|---|---|---|---|---|---|---|
| D7 [22] | 7 | 4 | 1 | 38.5 | 62.000 | 16.390 |
| D9 [22] | 9 | 8 | 1 | 38.5 | 31.000 | 10.200 |
| D33 [27] | 33 | 37 | 1 | 12.66 | 3.715 | 2.300 |
| DF3 [28] | 16 | 13 | 3 | 38.5 | 28.700 | 8.900 |
| DF6 [29] | 44 | 38 | 6 | 38.5 | 59.300 | 17.800 |
| DF8 [24] | 77 | 33 | 8 | 10.5 | 33.587 | 10.733 |

The data of the aforementioned cases are published in [30] . All the cases enable us to obtain a success optimal power flow (OPF) solution by the primal-dual interior point solver (MIPS) of MATPOWER [25]. For alternating current (AC) OPF, MIPS can usually provide a feasible power flow for the entire system and to some extent indicates the settings of the test cases are reasonable for OPF calculation.

### B. Generating T&D testbeds

The basic idea of generating an integrated T&D testbed is replacing the original aggregated loads of a TS by detailed DSs. Typically, the TS and a DS are connected through a distribution substation, and in most cases, the low-voltage busbar of a distribution substation is usually defined as the boundary bus [15]. Accordingly, the generating procedure started from the TS side is detailed below:

1） Selecting the buses that are proposed to connect DSs. Then, based on the scale of the original aggregated load,

selecting one or several feeders of a DS or entire DSs with a similar demand level. The demand levels are defined as the scope of the aggregated active and reactive load connected to a transmission bus.

2） Using tie-lines, one or two newly-defined transformers and a boundary bus [15] to represent a distribution substation that ensures the continuity between the TS and DSs (as shown in Fig. 1). All the feeders and DSs that are used to replace the common aggregated load of the TS are connected to the same boundary bus.

3） For a selected feeder or DS, the original slack bus is replaced by the connected boundary bus. The transformers with specified impedance and ratio are taken into account through the branches connecting the original transmission bus and the boundary bus.

4） Finishing all such replacement, a joint T&D test bed has been constructed. When this process is accomplished in MATLAB, the cases can be directly used for power flow (PF) and OPF simulations through MATPOWER. The data of the newly-generated T&D cases can also be exported in MATPOWER format or converted into a standard mathematical optimization format [31].

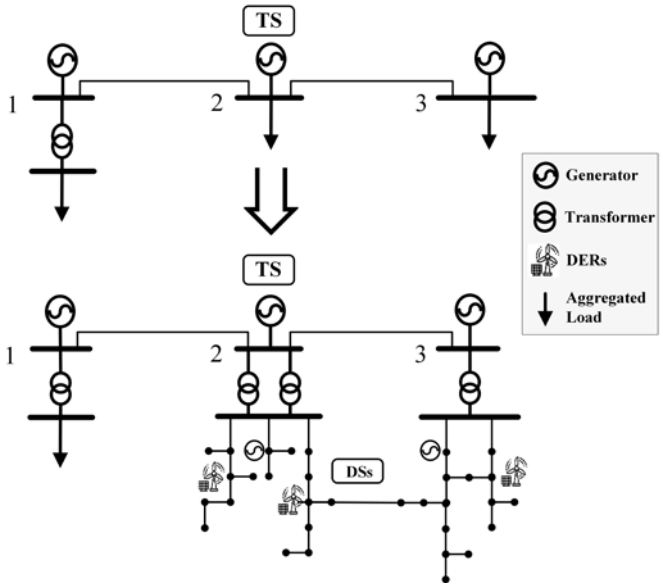


Fig. 1. Aggregated loads of the TS are replaced by detailed DSs.

The reasonable solutions obtained from MATPOWER can certainly prove the effectiveness of a newly-generated T&D testbed, and which can be further applied in the analysis of TSO-DSO interaction and coordination.

## III. T&D Benchmarks

In this section, four integrated T&D benchmarks varying in scale and characteristics were constructed based on the idea of replacing the aggregated loads of a TS by detailed DSs. The demand level (i.e., the scope of the aggregated active load (P) and reactive load (Q) connected to transmission buses) of the four TSs are given in TABLE III.

TABLE III
DEMAND SCOPES OF TS MODELS

| TS | P (MW) | Q (MVAR） |
|---|---|---|
| T6 | 30-62 | 8-25 |
| T14 | 3.5-94.2 | 1.6-19 |
| T30 | 2.2-30 | 0.7-30 |
| T118 | 2-277 | 1-113 |

The four benchmarks are T6-DF3, T30-DF6, T57-DF8 and T118-X, where the name before '-' represents the index of the specific TS presented in TABLE I, while after '-' is the index of DSs in TABLE II. The connection details are given in TABLE IV.

TABLE IV
SUMMARY OF T&D TEST SYSTEMS

| T&D Benchmarks | Bus ID with Boundary Bus | Number of Feeders/DSs |
|---|---|---|
| T6-DF3 | [3, 4, 5] | [6, 6, 6] |
| T30-DF6 | [5, 6, 8, 7, 9, 11] | [1, 1, 1, 1, 1, 1] |
| T57-DF8 | [18, 47] | [1, 1] |
| T118-X | [4, 32, 73, 92, 94, 95, 93, 100, 102, 103, 108, 109, 110, 118] | [1, 1, 2, 4, 4, 4, 1, 1, 1, 1, 1, 1, 1, 1] |

A more detailed introduction of each integrated T&D model are provided in the following sub-sections.

### A. *T6-DF3*

The integrated system T6-DF3 consists of the 6-bus TS (i.e. T6) and 3-feeder DS, i.e., DF3. The three feeders F1, F2, and F3 are connected with Buses #4, #5, and #6 of the TS. Moreover, there are 6 copies of the feeders connected to each boundary bus. This T&D model is designed to represent the traditional power system, wherein several feeders connected to the same boundary bus of the distribution substation, and in order to simplify computing, none of the tie-switches are closed, which means the DSs in this case is considered operating in a radial topology. The topology of DF3 is shown below [28].

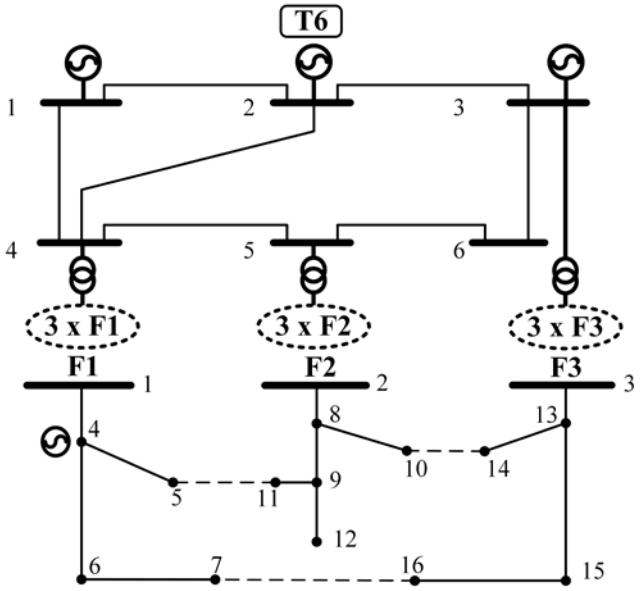


Fig. 2. DF3--the three-feeder DS.

### B. *T30-DF6*

The topology of the TS and DS that make up T30-DF6 are given separately by Fig.3 and Fig.4, respectively, and the topology of T30 is shown in Fig.3.

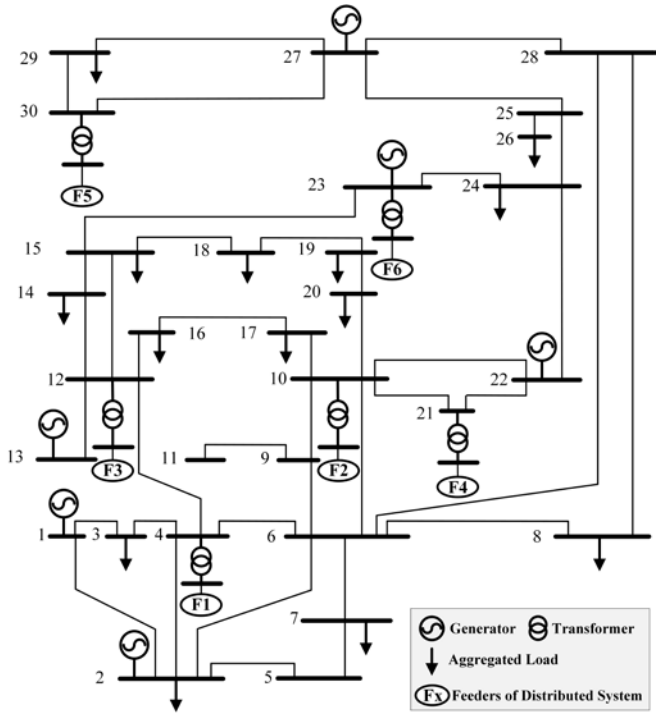


Fig. 3. The topology of T30.

In T30-DF6, the six feeders of DF6 are separately connected to transmission buses # 4, #10, #12, #21, #30, and #23 of the T30. While different from T6-DF3, two tie-switches in DF6 are closed to connect feeders that are connected to the different boundary buses. To be more specific, feeders F1 and F4 of DF6 are interconnected and so are feeders F2 and F3. This case is designed for the scenario, in which DSs are looped for reliability concerns. Fig.4 gives the looped topology of DF6.

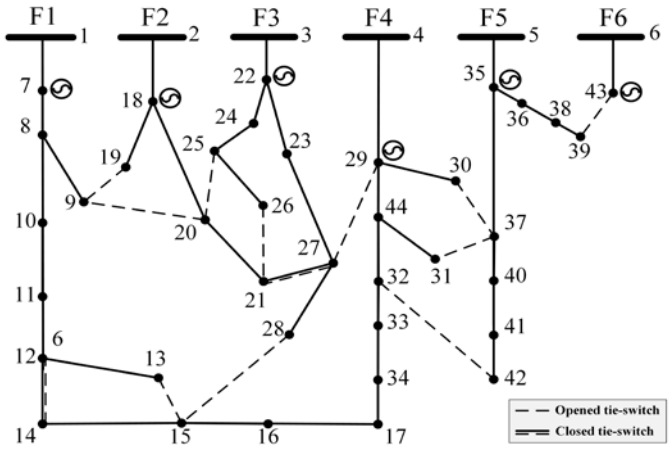


Fig. 4. The topology of DF6.

### C. T57-DF8

In T57-DF8, T57 is selected as TS and connected with two DF8 at transmission bus #18, #47, so there are three subsystems in this benchmark. The topology of IEEE57 is shown in Fig.5.

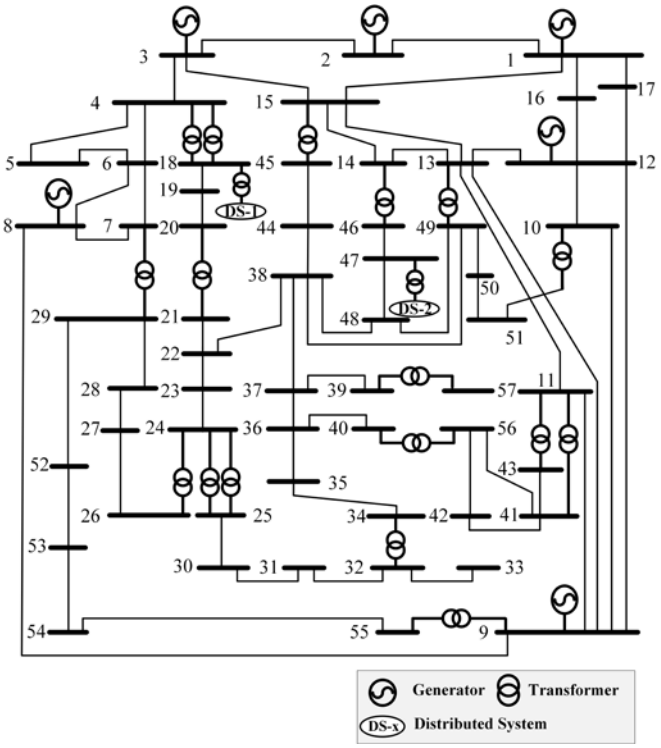


Fig. 5. The topology of T67.

It's worth mentioning that this T&D case is designed for the scenario when a mass of DERs are integrated into DSs. Therefore, DF8 includes two types of DERs, specifically, feeders F1-F4 are connected with controllable distribution generations (DGs), such as combined heat and power units and micro-turbines, to serving greater local demand. While the remaining feeders are serving residential demand, so that several small scale renewable energy sources, such as wind-turbine and rooftop photovoltaic (PV), are connected. The DF8 is modified based on that proposed in Ref [24], and for ensuring the reliability and stability of system operation, the 10 kV DS is fed from a 110kV supply point through two parallel-connected transformers. The diagram of DF8 is shown below.

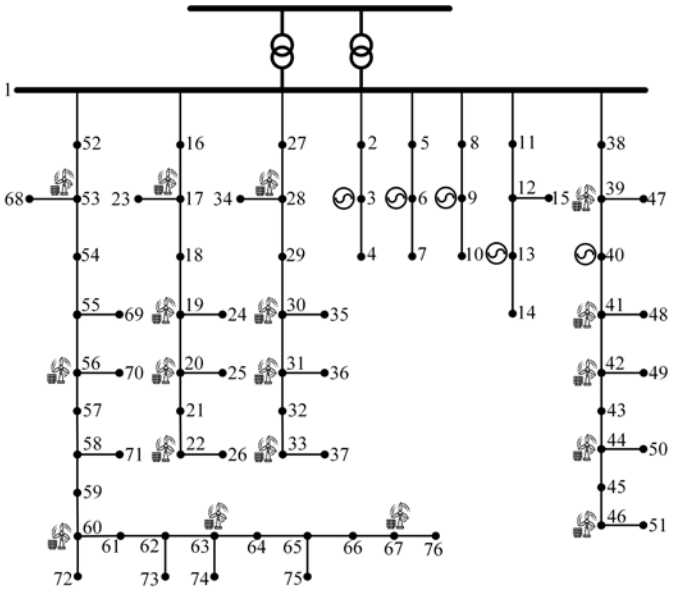

Fig. 6. The topology of DF8.

### D. T118-X

The T118-X is the largest test system designed in this paper, in which there are 14 boundary buses that are connected with 24 feeders of different DSs. As an integral T&D power system, there are 452 buses and 123 generators, and 69 of which are set to different types of DERs. The connection details are shown in the following table.

TABLE V
THE CONNECTION INFORMATION OF T118-X.

| Boundary Bus | Feeders/ DSs | Number |
|---|---|---|
| 4 | D7 | 1 |
| 32 | D9 | 1 |
| 73 | D33 | 2 |
| 92 | DF3-F2 | 4 |
| 93 | DF6-F3 | 1 |
| 94 | DF3-F3 | 4 |
| 95 | DF3-F1 | 4 |
| 100 | DF6-F3 | 1 |
| 102 | DF6-F3 | 1 |
| 103 | DF6-F3 | 1 |
| 108 | DF6-F3 | 1 |
| 109 | DF6-F3 | 1 |
| 110 | DF8 | 1 |
| 118 | DF8 | 1 |

## IV. SIMULATION RESULTS

All programs were coded and tested in MATLAB. We adopted the standard ACPF and ACOPF models for TSs and DSs, and the simulation results were executed by calling 'runpf.m' and 'runopf.m' of MATPOWER 7.1.b. Moreover, MIPS has been selected as the solver of OPF problems [32]. In order to validate the effectiveness of the newly-built T&D benchmarks, the results of PF and OPF for these integrated systems are provided in separate charts.

It is worth noting that since the T&D test systems are constructed by connecting separated DSs to TS, therefore, when connecting all the DSs to the TS, the original slack bus of a DS is no longer "slack" and has been replaced by the connected boundary bus. More than that, to improve understandability, the node names of DSs have been reorganized, which means the ID of other buses in DSs have been redefined based on the connection relations, and the method of renaming will be elaborated in subsequent subsections. Also, the power base in all cases is 100 MVA.

### A. T6-DF3

The integrated system T6-DF3 consists of the 6-bus TS and 18 radial feeders of DF3.

For the ACPF calculation, we adopted the standard Newton-Raphson method in the polar coordinate [32], and the ACPF results, including voltage magnitudes and angles, are given in TABLE VI. The explanation of the converted ID of distribution buses is that the first one (or first two in other cases) digit represents the bus ID of the connected transmission bus, and the following two digits are used to count the number of feeders connected to the same boundary bus, while the last two digits indicate the original bus ID in the previous DS.

TABLE VI
THE NODE VOLTAGE OF ACPF FOR T6-DF3

| Bus | Voltage (p.u.) | Angle (deg) | Bus | Voltage (p.u.) | Angle (deg) |
|---|---|---|---|---|---|
| 1 | 1.000 | 0.000 | 8(40101) | 0.973 | -15.933 |
| 2 | 1.000 | -0.403 | 40104 | 0.967 | -16.084 |
| 3 | 1.000 | -0.768 | 40105 | 0.963 | -16.237 |
| 4 | 0.997 | -1.070 | 40106 | 0.961 | -16.411 |
| 5 | 1.008 | 1.015 | 40107 | 0.961 | -16.436 |
| 6 | 1.004 | -0.362 | 9(50102) | 0.946 | 2.636 |
| 7(30103) | 1.012 | -14.463 | 50108 | 0.944 | 3.133 |
| 30113 | 1.005 | -14.587 | 50109 | 0.932 | 2.540 |
| 30114 | 1.004 | -14.634 | 50110 | 0.942 | 3.098 |
| 30115 | 1.002 | -14.721 | 50111 | 0.931 | 2.504 |
| 30116 | 1.000 | -14.749 | 50112 | 0.927 | 2.270 |

From the perspective of TS, the boundary buses seem like additional transmission buses (i.e., bus #7-#8), while they also the replacements of the previous slack buses in the feeders of DSs. Moreover, because of the existence of the distribution transformers connected to the transmission bus #4, #5 and #6, the voltages of newly-built boundary buses, i.e., #7, #8 and #9 are not same as those of the corresponding transmission buses in TS.

Table VII gives the results in terms of the active and reactive power flow over some branches. The highlighted branches indicate the newly-added tie-lines that connect TS and DSs.

TABLE VII
THE POWER FLOW RESULTS OF T6-DF3

| From | To | MW-flows | Mvar-flows | From | To | MW-flows | Mvar-flows |
|---|---|---|---|---|---|---|---|
| 1 | 2 | 2.819 | -3.397 | 30115 | 30116 | 2.102 | 0.902 |
| 1 | 4 | 9.093 | -2.891 | 8 | 40104 | 4.545 | 2.769 |
| 2 | 3 | 2.453 | -3.482 | 40104 | 40105 | 3.009 | 1.012 |
| 2 | 4 | 10.356 | -3.519 | 40104 | 40106 | 3.514 | 1.127 |
| 3 | 6 | -7.648 | -3.623 | 40106 | 40107 | 1.501 | 0.501 |
| 4 | 5 | -8.316 | -2.315 | 9 | 50108 | -2.746 | 4.299 |
| 5 | 6 | 7.722 | -4.214 | 50108 | 50109 | 10.221 | 2.666 |
| 3 | 7 | 25.098 | -4.520 | 50108 | 50110 | 1.002 | 0.502 |
| 7 | 30113 | 4.135 | 2.139 | 50109 | 50111 | 0.600 | 0.100 |
| 30113 | 30114 | 1.001 | 0.401 | 50109 | 50112 | 4.520 | 1.127 |
| 30113 | 30115 | 3.111 | 1.314 | | | | |

Besides, the results of ACOPF are listed in TABLE VIII, wherein the voltage magnitudes and angles obtained in ACOPF are notably different from those in ACPF.

TABLE VIII
THE NODE VOLTAGE FOR ACOPF OF T6-DF3

| Bus | Voltage (p.u.) | Angle (deg) | Bus | Voltage (p.u.) | Angle (deg) |
|---|---|---|---|---|---|
| 1 | 1.000 | 0.000 | 8 | 1.048 | -3.007 |
| 2 | 1.003 | -0.600 | 40104 | 1.047 | -2.839 |
| 3 | 1.001 | -1.807 | 40105 | 1.044 | -2.970 |
| 4 | 1.014 | -0.955 | 40106 | 1.042 | -3.118 |
| 5 | 1.011 | -5.015 | 40107 | 1.041 | -3.139 |
| 6 | 1.007 | -2.620 | 9 | 1.030 | -19.111 |
| 7 | 1.067 | -7.084 | 50108 | 1.023 | -19.256 |
| 30113 | 1.065 | -7.005 | 50109 | 1.012 | -19.760 |
| 30114 | 1.064 | -7.048 | 50110 | 1.021 | -19.286 |
| 30115 | 1.061 | -7.126 | 50111 | 1.012 | -19.791 |
| 30116 | 1.060 | -7.150 | 50112 | 1.007 | -19.989 |

TABLE IX compares the results in terms of the active and reactive power outputs of generators in the different calculations. For simplicity, "P" and "Q" are used as the abbreviations of "active power" and "reactive power" in the following tables.

TABLE IX
THE NODE VOLTAGE OF POWER FLOW OF T6-DF3

| T6-DF3 | Bus ID | P (MW) | | Q (Mvar) | |
|---|---|---|---|---|---|
| | | PF | OPF | PF | OPF |
| TS | 1 | 11.912 | 10.000 | -6.288 | -15.690 |
| | 2 | 10.000 | 5.000 | -7.585 | -15.578 |
| | 3 | 15.000 | 5.000 | -10.645 | -24.999 |

| | | | | | |
|---|---|---|---|---|---|
| DF3-F1 | 30104, 30204, 30304<br>30404, 30504, 30604 | 1.000 | 5.000 | 0.000 | 0.578 |
| DF3-F2 | 40108, 40208, 40308<br>40408, 40508, 40608 | 4.000 | 9.949 | 0.000 | 0.329 |
| DF3-F3 | 50113, 50213, 50313<br>50413, 50513, 50613 | 18.000 | 10.797 | 0.000 | 2.268 |

Notably, from the above tables, all the results of PF and OPF we obtained are reasonable, as there were no violations of operational constraints. While, unlike OPF calculation, all generator limits, branch flow limits or voltage magnitude limits are ignored by the ACPF solvers of MATPOWER [32], so that when parameters are changed, some violations may occur, and more actions, such as bus type switching should be applied to obtain a reasonable PF solution.

### *B. T30-DF6*

The integrated system T30-DF6 is composed of the T30 and the 6-feeder meshed DS, i.e. the DF6. The ACPF results of T30-DF6 are shown in TABLE X.

TABLE X
THE POWER FLOW RESULTS OF T30-DF6

| Bus | Voltage (p.u.) | Bus | Voltage (p.u.) | Bus | Voltage (p.u.) |
|---|---|---|---|---|---|
| 1 | 1.000 | 26 | 1.003 | 100221 | 1.006 |
| 2 | 1.030 | 27 | 1.030 | 120322 | 1.000 |
| 3 | 1.009 | 28 | 1.009 | 120323 | 1.002 |
| 4 | 1.012 | 29 | 1.020 | 120324 | 0.994 |
| 5 | 1.014 | 30 | 1.019 | 120325 | 0.990 |
| 6 | 1.007 | 31(40101) | 1.015 | 120326 | 0.986 |
| 7 | 1.001 | 32(100202) | 1.033 | 120327 | 1.003 |
| 8 | 0.995 | 33(120303) | 1.008 | 120328 | 1.001 |
| 9 | 1.013 | 34(210404) | 1.006 | 210429 | 1.000 |
| 10 | 1.017 | 35(300505) | 1.016 | 210430 | 0.999 |
| 11 | 1.013 | 36(230606) | 1.015 | 210431 | 0.989 |
| 12 | 1.019 | 40107 | 1.010 | 210432 | 0.985 |
| 13 | 1.030 | 40108 | 1.003 | 210433 | 0.976 |
| 14 | 1.010 | 40109 | 1.003 | 210434 | 0.973 |
| 15 | 1.013 | 40110 | 0.992 | 300535 | 1.010 |
| 16 | 1.011 | 40111 | 0.980 | 300536 | 1.007 |
| 17 | 1.010 | 40112 | 0.973 | 300537 | 1.004 |
| 18 | 1.002 | 40113 | 0.970 | 300538 | 1.002 |
| 19 | 0.999 | 210414 | 0.971 | 300539 | 1.001 |
| 20 | 1.002 | 210415 | 0.970 | 300540 | 0.993 |
| 21 | 1.026 | 210416 | 0.970 | 300541 | 0.985 |
| 22 | 1.030 | 210417 | 0.971 | 300542 | 0.983 |
| 23 | 1.030 | 100218 | 1.030 | 230643 | 1.010 |
| 24 | 1.019 | 100219 | 1.028 | 210444 | 0.990 |
| 25 | 1.020 | 100220 | 1.011 | | |

For clarify, in this case, the two digits in the middle of the bus ID represent the feeder ID, i.e., the nomenclature here is that in '40101', '4' is transmission bus ID, '01' means the F1 of DF6, and the last two digits '01' is the previous bus ID in the DS. Meanwhile, as shown in TABLE X, all the obtained voltage magnitudes are between the operational lower and upper limits.

Then, TABLE XI compares the active power flow at some branches obtained by ACPF and DCPF. Although there are some differences, the changing trends in both cases are similar. The highlighted branches are tie-lines and closed tie-switches.

TABLE XI
THE POWER FLOW RESULTS OF T30-DF6

| Branch | MW-Flows | | Branch | MW-Flows | |
|---|---|---|---|---|---|
| i-j | ACPF | DCPF | i-j | ACPF | DCPF |
| 1-2 | -16.510 | -18.739 | 10-17 | 4.272 | 4.329 |
| 1-3 | 0.303 | -0.831 | 10-21 | -12.524 | -12.658 |
| 2-4 | 5.516 | 4.925 | 10-22 | -7.805 | -7.938 |
| 3-4 | -2.109 | -3.231 | 21-22 | -14.608 | -15.231 |
| 2-5 | 8.433 | 7.988 | 15-23 | -11.036 | -11.038 |
| 2-6 | 8.360 | 7.618 | 22-24 | -0.916 | -1.579 |
| 4-6 | 14.198 | 13.351 | 23-24 | 6.954 | 7.162 |
| 5-7 | 8.381 | 7.988 | 24-25 | -2.779 | -3.117 |
| 6-7 | 14.546 | 14.812 | 25-26 | 3.544 | 3.500 |
| 6-8 | 23.288 | 23.241 | 25-27 | -6.339 | -6.617 |
| 6-9 | -5.461 | -6.395 | 28-27 | -13.701 | -13.793 |
| 6-10 | -3.121 | -3.654 | 27-29 | 3.527 | 3.388 |
| 9-11 | 0.000 | 0.000 | 27-30 | 3.299 | 3.112 |
| 9-10 | -5.461 | -6.395 | 29-30 | 1.100 | 0.988 |
| 4-12 | -14.627 | -14.184 | 8-28 | -6.824 | -6.759 |
| 12-13 | -37.000 | -37.000 | 6-28 | -6.824 | -7.035 |
| 12-14 | 4.939 | 4.813 | 4-40101 | 3.767 | 2.527 |
| 12-15 | 7.444 | 7.494 | 10-100202 | 1.357 | 0.262 |
| 12-16 | 8.329 | 8.171 | 12-120303 | 1.662 | 2.338 |
| 14-15 | -1.292 | -1.387 | 21-210404 | 2.019 | 2.573 |
| 16-17 | 4.768 | 4.671 | 30-300505 | 4.363 | 4.100 |
| 15-18 | 8.947 | 8.945 | 23-230606 | 1.083 | 1.000 |
| 18-19 | 5.660 | 5.745 | 40112-210414 | 0.995 | 0.027 |
| 19-20 | -3.859 | -3.755 | 100221-120327 | -0.394 | -1.338 |
| 10-20 | 6.118 | 5.955 | | | |

Moreover, in this case, the operation cost of reactive power has also been taken into account. From the results shown in the following table, it is easy to make a conclusion that after the OPF calculations, to meet the same active demand, the real power outputs of generators in both cases were roughly the same, while not only the power losses, but also the generation cost regarding the reactive power in ACOPF has been taken into account [32].

TABLE XII
THE NODE VOLTAGE OF POWER FLOW OF T6-DF3

| T6-DF3 | Bus ID | P (MW) | | Q (Mvar) | |
|---|---|---|---|---|---|
| | | ACOPF | DCOPF | ACOPF | DCOPF |
| TS | 1 | 15.272 | 20.352 | 4.941 | - |
| | 2 | 27.382 | 28.241 | 3.393 | - |
| | 13 | 0.000 | 0.000 | 2.489 | - |
| | 22 | 40.919 | 27.007 | 2.171 | - |
| | 23 | 25.050 | 30.000 | 1.180 | - |
| | 27 | 39.999 | 40.000 | 2.326 | - |
| DF6-F1 | 40107 | 0.000 | 0.000 | 1.200 | - |
| DF6-F2 | 100218 | 5.000 | 5.000 | 1.500 | - |
| DF6-F3 | 120322 | 11.000 | 11.000 | 3.500 | - |
| DF6-F4 | 210429 | 13.000 | 13.000 | 3.500 | - |
| DF6-F5 | 300535 | 13.000 | 13.000 | 1.509 | - |
| DF6-F6 | 230643 | 5.000 | 5.000 | 0.758 | - |
| Cost ($) | | 2806.308 | 2739.421 | 26.593 | - |

### *C. T57-DF8*

Since T57-DF8 is specially designed for the scenarios with high DER penetration, among the generators, 42 out of the 49 generators were set to different types of renewable energy sources (RESs), and the outputs of which are intermittent and unpredictable. Therefore, in this case the parameters of the DF8 that connected to the different boundary buses were not exactly the same. The ACPF results for T57-DF8 in terms of the voltage magnitudes are shown in Fig.7, which intuitively illustrates that the obtained voltage magnitudes of all buses were within the operational ranges.

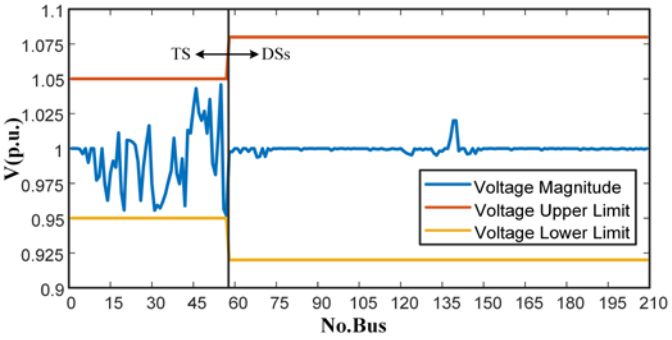


Fig. 7. The voltage magnitudes of ACPF for T57-DF8.

Moreover, the ACOPF results, regarding the voltage magnitudes and active generations, for TS and DSs in case T57-DF8 are shown in Fig.8 and Fig.9, respectively.

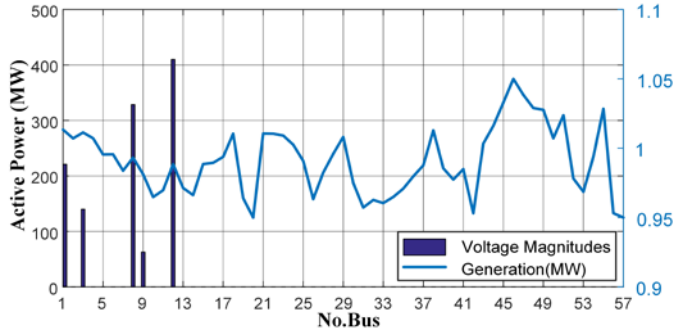


Fig. 8. The voltage magnitudes and active generations of T57

When connecting all the DSs to the TS, the bus numbers of DSs have been reordered in the connecting order. As shown in Fig.9, the generations of the RES directly determined the states, i.e. voltage magnitudes, of DSs, which can also place impacts on the operation of TS. Therefore, especially in high-level RESs penetrations scenarios, the coordination between separated systems and accurate prediction will play more critical roles.

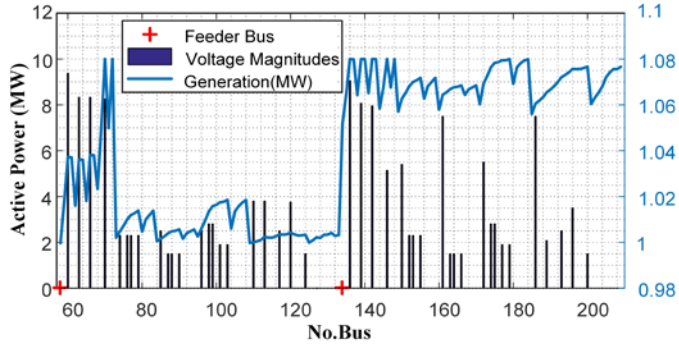


Fig. 9. The voltage magnitudes and active generations of DSs.

Notably, the capacities of generators in DSs are roughly less than 10 MW, so that the types of distributed generation units can be freely modified to combined heat and power units, solar, wind, fuel cells and so on [33].

### *D. T118-X*

The T118-X is the largest test system, which consists of the IEEE118 TS and 24 feeders or DSs, so there are 25 subsystems in this integral T&D system. Moreover, all the tie-switches are opened and the DSs are in radial topologies. The ACPF results for the voltage magnitudes of 452 buses are shown in Fig.7, in which the curve represents the obtained voltage magnitudes of all buses was just between the operational limits.

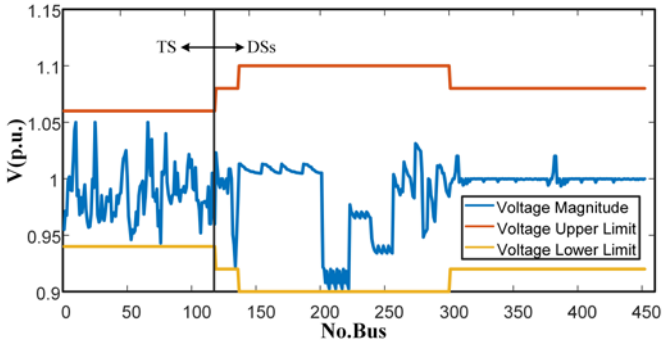


Fig. 10. The voltage magnitudes of ACPF for T118-X.

Besides, TABLE XIII gives the ACOPF results of this large-scale benchmark in terms of the voltage magnitudes and power injections at the transmission buses that connected with boundary buses.

TABLE XIII
ACOPF RESULTS OF CASE T118-X

| Boundary Bus | Voltage (p.u.) | Active Power (MW) | Reactive Power (MW) |
|---|---|---|---|
| 4 | 1.056 | 0.316 | 5.364 |
| 32 | 1.041 | -5.536 | 3.140 |
| 73 | 1.026 | -0.535 | 2.663 |
| 92 | 1.057 | -19.009 | 5.293 |
| 94 | 1.048 | 0.441 | 0.494 |
| 95 | 1.044 | -5.910 | 0.546 |
| 93 | 1.052 | 0.080 | 1.301 |
| 100 | 1.049 | 1.265 | 0.695 |
| 102 | 1.052 | 1.116 | 1.215 |
| 103 | 1.039 | 2.961 | 1.805 |
| 108 | 1.018 | 0.000 | 0.030 |
| 109 | 1.016 | 2.618 | 1.184 |
| 110 | 1.013 | -52.197 | 7.955 |
| 118 | 1.016 | -52.104 | 8.546 |

It was found that when the connected DSs integrate more DERs than their local demands, there may be reverse power flows at the corresponding boundary buses, which may place challenges and impacts on the operation of TS. Therefore, in the face of such changeable boundary states, the operators of separated systems should work together to explore the potential of interactions for a better dispatch of the entire power system.

## V. CONCLUSION

In this paper, some benchmarks for the integrated T&D system have been proposed. The data of the cases are published to the public for researches focus on the coordination of TS and DSs. All benchmarks proposed in this paper are simulated under MATPOWER, and the obtained simulation results certainly validate the effectiveness of the new-built benchmarks.

However, since the ACOPF problems are nonconvex, the solution obtained by MIPS was a local optimum, and there is no information to estimate whether the obtained local optimum is the global optimum, so that it actually provided an upper bound of the ACOPF solution, and there might be other local optimum points founded by other algorithms.

More improvements can be made based on the current versions of the models, such as adding more practical flow

limits and generation capacities, and more precisely large-scale integrated T&D systems should also be developed in future studies.

## REFERENCES


[1] M. Birk, J P. Chaves Ávila, T. Gómez, et al. “TSO/DSO coordination in a context of distributed energy resource penetration”, *EEIC*, 2016.

[2] MT "Coordination of Transmission and Distribution Operations in a High Distributed Energy Resource Electric Grid." 2017.

[3] P. Aristidou, G. Valverde and T. Van Cutsem, "Contribution of Distribution Network Control to Voltage Stability: A Case Study," in IEEE Transactions on Smart Grid, vol. 8, no. 1, pp. 106-116, Jan. 2017.

[4] M. Heleno, R. Soares, J. Sumaili, R. Bessa, L. Seca, and M. Matos, “Estimation of the flexibility range in the transmission-distribution boundary,” in IEEE Eindhoven PowerTech, Jun. 2015, pp. 1–6.

[5] ENTSO (European Network of Transmission System Operators), “General guidelines for reinforcing the cooperation between TSOs and DSOs,” Nov. 9, 2015. [Online]. Available: https://www.entsoe.eu.

[6] Z. Li, Distributed Transmission-Distribution Coordinated Energy Management Based on Generalized Master-Slave Splitting Theory, 2018, ch.1, pp. 1–15.

[7] J. Villar, R. Bessa, M.Matos,”Flexibility products and markets: Literature review,” in Electric Power Systems Research,Vol. 154, pp. 329-340, 2018.

[8] I. J. Perez-Arriaga, "The Transmission of the Future: The Impact of Distributed Energy Resources on the Network," in IEEE Power and Energy Magazine, vol. 14, no. 4, pp. 41-53, July-Aug. 2016.

[9] A. Zegers and H. Brunner, “TSO-DSO interaction: An overview of current interaction between transmission and distribution system operators and an assessment of their cooperation in smart grids,” Int. Smart Grid Action Netw. Discussion Paper, Sep. 2014.

[10] ACER (agency for the cooperation of energy regulation), ““A bridge to 2025” publication proposals for future roles of DSOs,” [Online] Available: https://acer.europa.eu.

[11] European Commission “ Workshop on digitizing the energy value chain,” Feb, 26, 2018. [Online] Available: https://ec.europa.eu.

[12] Gerard, H., Israel, E., Puente, R., Six, D, “Coordination between transmission and distribution system operators in the electricity sector: A conceptual framework,” in Util. Policy. vol. 50, pp. 40-48, 2018.

[13] CEER (Council of European Energy Regulators) “CEER Position Paper on the Future DSO and TSO Relationship,” Sep, 21, 2016. [Online] Available: https://www.ceer.eu.

[14] H. Sun, Q. Guo, B. Zhang, Y. Guo, Z. Li, and J. Wang, “Master-slave splitting based distributed global power flow method for integrated transmission and distribution analysis,” IEEE Trans. Smart Grid, vol. 6, no. 3, pp. 1484–1492, May 2015.

[15] Z. Li, Q. Guo, H. Sun and J. Wang, "Coordinated Transmission and Distribution AC Optimal Power Flow," in IEEE Transactions on Smart Grid, vol. 9, no. 2, pp. 1228-1240, March 2018.

[16] Z. Li, Q. Guo, H. Sun, and J. Wang, ″Coordinated economic dispatch of coupled transmission and distribution systems using heterogeneous decomposition,″ IEEE Trans. Power Syst., vol. 31, no. 6, pp. 4817−4830, Nov. 2016.

[17] J. Yu, Z. Li, Y. Guo and H. Sun, "Decentralized Chance-Constrained Economic Dispatch for Integrated Transmission-District Energy Systems," in IEEE Transactions on Smart Grid.

[18] Y. Guo, L. Tong, W. Wu, B. Zhang and H. Sun, "Coordinated Multi-Area Economic Dispatch via Critical Region Projection," in IEEE Transactions on Power Systems, vol. 32, no. 5, pp. 3736-3746, Sept. 2017.

[19] Z. Li, J. Wang, H. Sun, and Q. Guo, “Transmission contingency analysis based on integrated transmission and distribution power flow in smart grid,” IEEE Trans. Power Syst, vol. 30, no. 6, pp. 3356–3367, Nov. 2015.

[20] Z. Li, J. Wang, H. Sun and Q. Guo, "Transmission Contingency Screening Considering Impacts of Distribution Grids," in IEEE Transactions on Power Systems, vol. 31, no. 2, pp. 1659-1660, March 2016.

[21] R. Venkatraman, S. K. Khaitan, et al., "Dynamic Co-Simulation Methods for Combined Transmission-Distribution System With Integration Time Step Impact on Convergence," in IEEE Transactions on Power Systems, vol. 34, no. 2, pp. 1171-1181, March 2019.

[22] A. Kargarian and Y. Fu, "System of Systems Based Security-Constrained Unit Commitment Incorporating Active Distribution Grids," in IEEE Transactions on Power Systems, vol. 29, no. 5, pp. 2489-2498, Sept. 2014.

[23] P. Aristidou, G. Valverde and T. Van Cutsem, "Contribution of Distribution Network Control to Voltage Stability: A Case Study," in IEEE Transactions on Smart Grid, vol. 8, no. 1, pp. 106-116, Jan. 2017.

[24] N. Pilatte, P. Aristidou and G. Hug, "TDNetGen: An Open-Source, Parametrizable, Large-Scale, Transmission, and Distribution Test System," in IEEE Systems Journal, vol. 13, no. 1, pp. 729-737, March 2019.

[25] R. D. Zimmerman and C. Murillo-Sánchez, MATPOWER User’s Manual. [Online]. Available: http://www.pserc.cornell.edu/matpower/.

[26] A. Azizivahed, M. Barani, S. Razavi, S. Ghavidel, L. Li and J. Zhang, "Energy storage management strategy in distribution networks utilised by photovoltaic resources," in IET Generation, Transmission & Distribution, vol. 12, no. 21, pp. 5627-5638, 2018.

[27] M. E. Baran, F. F. Wu, "Network reconfiguration in distribution systems for loss reduction", IEEE Trans. Power Del., vol. 4, no. 2, pp. 1401-1407, Apr. 1989.

[28] Civanlar S, Grainger JJ, Yin H et al, “Distribution feeder reconfiguration for loss reduction,” in IEEE Trans Power, Del 3(3):1217–1223, 1988.

[29] Wagner TP, Chikhani AY, Hackam R “ Feeder reconfiguration for loss reduction: An application of distribution automation,” in IEEE Trans Power Del 6(4):1922–1933, 1991.

[30] Data for test systems. [Online]. Available: https://figshare.com/s/d74a909d36e88b73bb13

[31] C. Josz, S. Fliscounakis, J. Maeght, and P. Panciatici, “AC Power Flow Data in MATPOWER and QCQP Format: iTesla, RTE Snapshots, and PEGASE,” eprint arXiv:1603.01533, pp. 1–7, 3 2016.

[32] R. D. Zimmerman, C. E. Murillo-Sanchez and R. J. Thomas, "MATPOWER: Steady-State Operations, Planning, and Analysis Tools for Power Systems Research and Education," in IEEE Transactions on Power Systems, vol. 26, no. 1, pp. 12-19, Feb. 2011.

[33] P. P. Barker and R. W. De Mello, "Determining the impact of distributed generation on power systems. I. Radial distribution systems," 2000 Power Engineering Society Summer Meeting (Cat. No.00CH37134), Seattle, WA, 2000, pp. 1645-1656 vol. 3.